Comparison of inversion recovery gradient echo with inversion recovery fast spin echo techniques for magnetic resonance imaging detection of navicular bone marrow lesions in horses

Julien Olive, DMV, MSc; Thibault Vila, DMV; Nicolas Serraud, DMV

Objective—To compare navicular bone marrow lesion (BML) conspicuity in the feet of horses as determined via 2 fat-suppressed MRI techniques, including standard short tau inversion recovery (STIR) and inversion recovery gradient echo (IRGE).

Sample—Feet (n = 150) of horses with lameness referable to the distal portion of the digit.

Procedures—STIR and IRGE sequences were obtained prospectively in all feet with a standing low-field equine MRI system. Presence of a BML was ascertained by identification of a characteristic combination of marrow alterations in T1-weighted, T2*-weighted, T2-weighted, and STIR images. Signal-to-noise and contrast-to-noise ratios were calculated on STIR and IRGE sequences in 56 feet with a navicular BML.

Results—Signal-to-noise and contrast-to-noise ratios of both sequences correlated linearly (r = 0.87 and r = 0.92, respectively) but were significantly higher for STIR images (mean ± SD, 22.6 ± 12.7 and 12.4 ± 11.4, respectively), compared with IRGE images (13.7 ± 8.0 and 5.9 ± 7.2, respectively).

Conclusions and Clinical Relevance—Results suggested that the IRGE sequence revealed BMLs significantly less conspicuously, compared with the standard STIR sequence. The 2 techniques cannot be used interchangeably, and IRGE is therefore not recommended as the sole fat-suppressed sequence for routine equine standing MRI protocols. (*Am J Vet Res* 2013;74:232–238)

The STIR sequence is part of routine orthopedic MRI protocols, especially in low-field systems in which frequency-selective fat saturation is not achievable.[1] One of the paramount objectives of a STIR sequence is detection of BMLs that appear on that sequence as ill-defined hyperintensities in the normally hypointense bone marrow spaces of trabecular bone.[2–4] Bone marrow lesions may be found in a wide variety of pathological conditions, including direct bone trauma or contusion, subchondral damage and osteoarthritis, enthesiopathy, osteomyelitis, and bone neoplasia.[5] The precise clinical importance of BMLs in horses is not yet entirely elucidated because lameness is often multifactorial,[6] and BMLs may or may not be closely related to the lameness status in horses.[7–9] Nonetheless, BML detection is still considered an important aspect of orthopedic MRI examinations,[6] especially at the time of innovative surgical treatment investigations.[10]

Abbreviations

BML	Bone marrow lesion
CNR	Contrast-to-noise ratio
GRE	Gradient recalled echo
IRGE	Inversion recovery gradient echo
ROI	Region of interest
SI	Signal intensity
SNR	Signal-to-noise ratio
STIR	Short tau inversion recovery fast spin echo
TE	Time to echo
TR	Time to repetition

Most commonly, a STIR sequence is acquired via the fast spin echo technique.[1] This sequence requires a preliminary 180° inversion pulse. By choosing an appropriate time of inversion so that protons in fat have no longitudinal magnetization at the time of the 90° excitation pulse, no signal is registered from the fat. Multiple echoes are subsequently registered, allowing multislice imaging.[1] Especially in standing horses, motion during the echo train sampling and between 2 excitations at the same location may have deleterious effects on image quality. The STIR sequence can occasionally

Received March 27, 2012.
Accepted June 25, 2012.
From the Diagnostic Imaging Department, Faculty of Veterinary Medicine, University of Montreal, St-Hyacinthe, QC J2S 7C6, Canada, and Teleradiology Service, Capinghem, 59160, France (Olive);
Clinique Vétérinaire Equine de Chantilly, 20bis Rue Victor Hugo, 60500 Chantilly, France (Vila); and Imavet, 3910 Route de Launac, 31330 Grenade-sur-Garonne, France (Serraud).
The authors thank Dr. Guy Beauchamp for statistical analyses and Dr. Steve Roberts for providing manufacturer details about sequence conception.
Address correspondence to Dr. Olive (julien_olive_veto@hotmail.com).

be challenging to acquire in a standing sedated horse but remains the standard for identification of BMLs.

Alternatively, the inversion recovery principle can be applied before a gradient echo sequence to similarly obtain fat signal suppression.[11–13] As currently optimized on a widely available standing equine MRI system,[a] the IRGE sequence (named STIR GRE by the manufacturer) has only 1 echo/TR and a single excitation, which make this sequence theoretically more robust in response to motion. It is the authors' clinical impression that IRGE sequences are obtained much more frequently with fewer motion artifacts, compared with the standard STIR sequence. It may be tempting to switch from the STIR method to the IRGE method to improve image quality obtained with a standing MRI system, in which horses are most likely to move. However, a gradient echo–based sequence may result in lower BML conspicuity and this has not been investigated. Indeed, the lower T2 weighting caused by the shorter time to echo and the risk of susceptibility artifacts inherent to the GRE technique may affect its capability to detect BMLs.

The purpose of the study reported here was to prospectively compare relative conspicuity of IRGE and STIR sequences for navicular BMLs in MRI of the clinical equine foot by calculating their SNR and CNR. These are considered the most important image-quality parameters and have the major advantage of independence from observer performance.[1] It was hypothesized that IRGE images would have inferior lesion conspicuity, compared with STIR images.

Materials and Methods

Animals—Horses selected for the study had lameness localized to the foot by use of either perineural or intrasynovial analgesia, standing MRI examination of a foot, and at least sagittal IRGE and sagittal STIR sequences of diagnostic quality, transverse STIR sequences of diagnostic quality, or both as part of the imaging protocol.

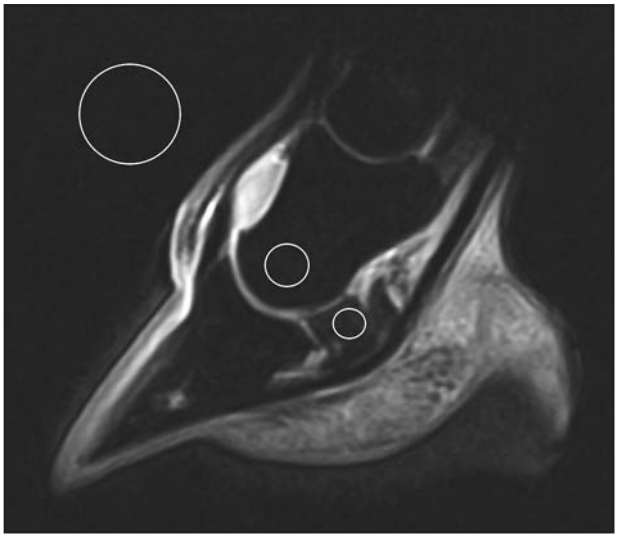

Figure 1—Example of a sagittal IRGE MRI image of a horse with mild diffuse navicular BMLs. Circles indicate positions of ROIs in the navicular bone (0.4 cm^2), middle phalanx (1.0 cm^2), and air (3 cm^2). In this example, SNR was 10.0 and CNR was 4.8.

Imaging—Images were obtained in 2 clinics with the same standardized foot protocol. Standard imaging parameters on the 0.27-T standing MRI unit[a] were as follows: inversion time, 75 milliseconds; flip, 90°; TE, 8 milliseconds; TR, 1,500 milliseconds; echo train length, 1; thickness, 5 mm; spacing, 0.6 mm; field of view, 18 cm; matrix, 160 × 160; number of excitations, 1; and scan time, 4.07 minutes for IRGE sequence and TI, 85 milliseconds; flip, 90°; TE, 27 milliseconds; TR, 2,910 milliseconds; echo train length, 5; thickness, 5 mm; spacing, 0.6 mm; field of view, 18 cm; matrix, 168 × 165; number of excitations, 2; and scan time, 3.77 minutes for STIR sequence.

A noncystic BML was considered present if a combination of bone marrow SI alterations was visible on the basis of other recommendations,[8,14] including reduced SI on 3-D T1-weighted gradient echo (GRE) images (TR, 23 milliseconds; TE, 7 milliseconds; and flip, 40°) with no markedly increased SI on T2-weighted fast spin echo images (TR, 2,125 milliseconds; TE, 84 milliseconds; and flip, 90°) to exclude cyst formations,

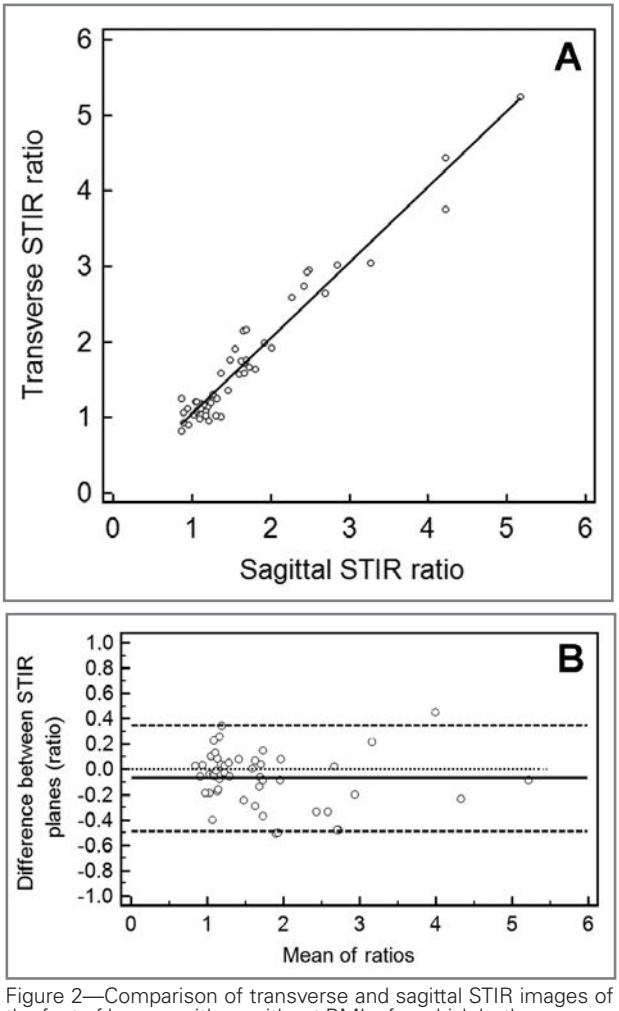

Figure 2—Comparison of transverse and sagittal STIR images of the feet of horses with or without BMLs for which both sequences were acquired. A—Scatterplot of transverse STIR SI ratio versus sagittal STIR SI ratio. Notice excellent correlation. B—Bland-Altman difference plot of SI ratio measurements in sagittal and transverse STIR images, indicating minimal bias according to the imaging plane. Dotted line indicates zero bias, black line indicates level of bias, and dashed lines indicate 95% limits of agreement.

Table 1—Mean ± SD simple ratios, SNRs, and CNRs for equine feet with and without a navicular BML.

	No BML	BML		
Variable	**Signal ratio**	**Signal ratio**	**SNR**	**CNR**
Sagittal IRGE	1.02 ± 0.12 (n = 94)	1.82 ± 1.03 (n = 56)	13.7 ± 8.0 (n = 56)	5.9 ± 7.2 (n = 56)
Sagittal STIR	1.07 ± 0.15 (n = 22)	2.34 ± 1.19 (n = 27)	21.7 ± 12.3 (n = 27)	12.2 ± 11.7 (n = 27)
Transverse STIR	1.09 ± 0.14 (n = 93)	2.27 ± 0.94 (n = 55)	22.3 ± 11.9 (n = 55)	12.1 ± 10.5 (n = 55)
Pooled STIR	1.09 ± 0.13 (n = 94)	2.30 ± 1.03 (n = 56)	22.6 ± 12.7 (n = 56)	12.4 ± 11.4 (n = 56)

a manifestation of phase cancellation artifact on out-of-phase T2*-weighted GRE images (TR, 135 milliseconds; TE, 13 milliseconds; and flip, 32°), and increased SI on STIR images. All of these additional sequences were acquired in all feet as part of the standardized protocol. The presence of BML was considered independent of size or location within the navicular bone.

Image analysis—The apparent mean SI of several ROIs was measured quantitatively in the same image with DICOM software[b]: a 1.0-cm^2 reference area in the central distal aspect of the middle phalanx trabecular bone, a 0.4-cm^2 area of BML or a central area of apparently normal navicular spongiosa, and a 3.0-cm^2 area of the background noise (**Figure 1**). These ROIs were placed with the help of other sequences to exclude compact bone and distal synovial invaginations. These signal intensities were measured on both transverse and sagittal STIR and on sagittal IRGE images. Horses with BML in the distal half of the middle phalanx were excluded from the study. All images were read retrospectively, and all measurements were made by the primary author.

A repeatability study of SI measurements was performed by use of all 3 sequences (sagittal IRGE and sagittal and transverse STIR) on a subset of 25 randomly selected horses, including 9 horses with a BML, to reproduce the proportion of affected horses. Measurements were made several weeks apart by the same evaluator.

To compare the relative navicular bone SI of horses with and without a BML, a simple ratio of the navicular bone marrow mean SI to the reference phalangeal mean SI was calculated. In horses with a BML, SNR and CNR were calculated with the following equations[15]:

$$\text{SNR} = \text{SI BML}/\text{noise}$$
$$\text{CNR} = (\text{SI BML} - \text{SI MP})/\text{noise}$$

where SI BML is the mean SI within the ROI drawn over the BML in the navicular bone, SI MP is the mean SI in the reference region of the middle phalanx, and noise is the SD of background air SI (Figure 1).

Statistical analysis—Repeatability of SI ratio measurements was evaluated via linear model regression. Bland-Altman bias plotting was used to test the agreement and limits of agreement of SI measurements between both planes of the STIR sequence, with the intent of pooling data. Correlation of SI ratios obtained from both STIR planes was also assessed with a linear regression model. Data were subsequently pooled by calculating the mean of SIs from both planes when applicable. Signal intensity ratios obtained with IRGE and STIR sequences from feet with and without BML were compared via the *t* test for unequal variances. The SNR and CNR obtained with IRGE and STIR sequences from feet with BML were compared via the paired *t* test. Correlation of SNR and CNR from IRGE and STIR sequences was tested with a linear regression model. Values of $P < 0.05$ were considered significant. Statistical analysis was performed with software.[c,d]

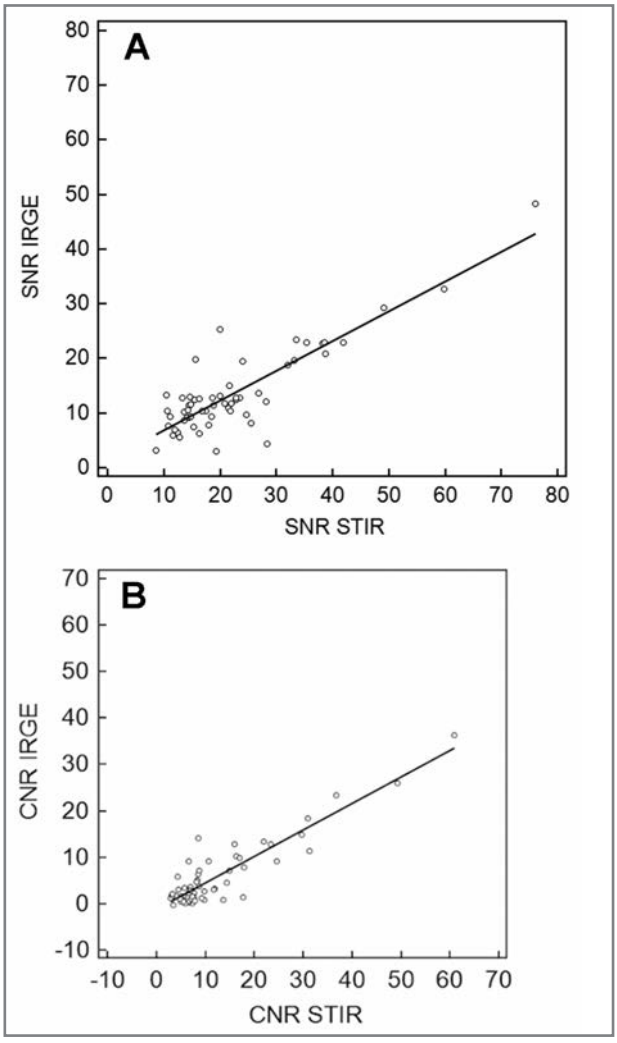

Figure 3—Correlation plots for IRGE SNR versus STIR SNR (A) and IRGE CNR versus STIR CNR (B) for images of the feet of horses with BMLs. Regression equations were $SNR_{IRGE} = 1.31 + 0.55 \times SNR_{STIR}$ and $CNR_{IRGE} = -1.33 + 0.58 \times CNR_{STIR}$.

Results

One hundred fifty-four feet were found in the database with the selected sequence acquisition inclusion

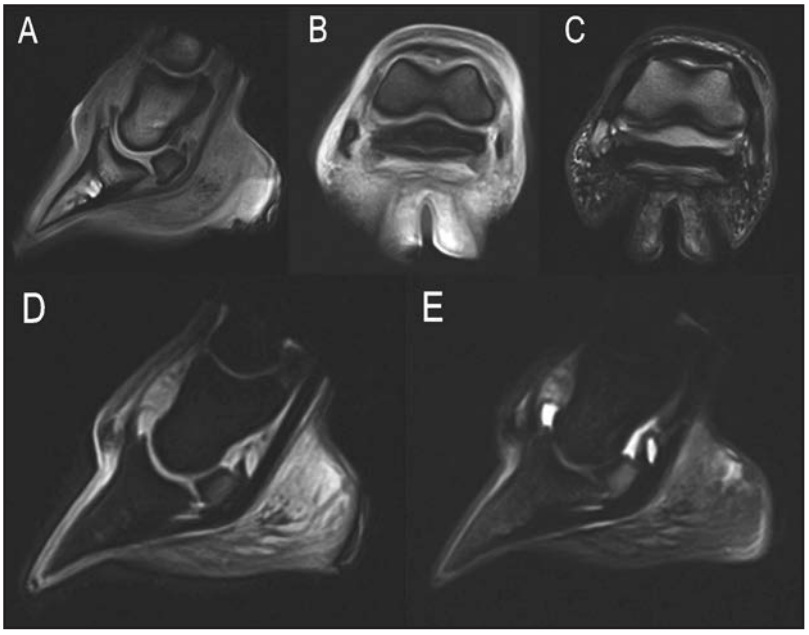

Figure 4—Corresponding sagittal T1-weighted GRE (A), transverse T2*-weighted GRE (B), transverse T2-weighted (C), sagittal IRGE (D), and sagittal STIR (E) images obtained via MRI of the same equine foot. Magnification of images D and E is 130%, compared with images A to C. Notice the variable visual conspicuity of the diffuse severe navicular BMLs in both inversion recovery sequences. Notice the characteristic combination of marrow alterations in T1-weighted GRE (moderately decreased SI), T2*-weighted GRE (multifocal signal voids consistent with phase cancellation artifact), and T2-weighted (diffuse mild increased SI but no cystic lesion) images. Contrast-to-noise ratio was 30 in STIR and 15 in IRGE images in this example.

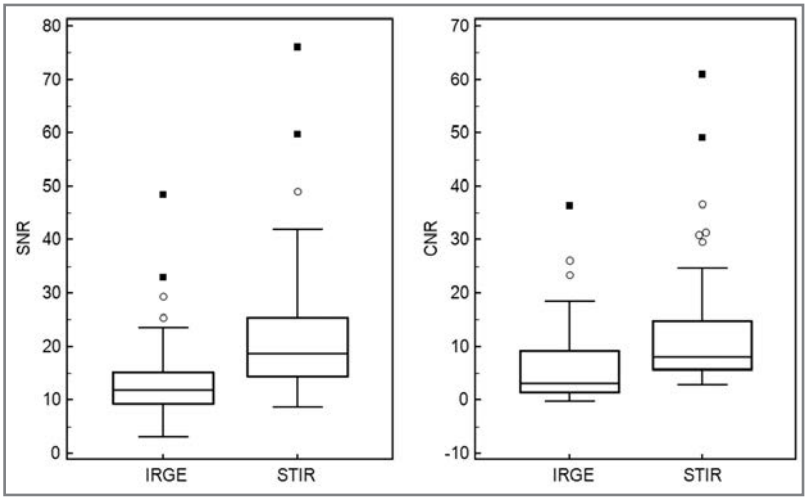

Figure 5—Box plots of SNRs and CNRs for IRGE and STIR sequences obtained via MRI of horses with BML. Boxes represent limits of the upper (Q3) and lower (Q1) quartiles, the mid horizontal lines represent the median, horizontal bars represent the lower or upper quartile minus or plus 1.5 times the interquartile range, and white circles represent outlying values (beyond the horizontal bars). Black squares represent extreme outlying values (less than or greater than the lower or upper quartile minus or plus 3 times the interquartile range).

criteria. Four feet were excluded because of the presence of a BML in the distal half of the middle phalanx; therefore, 150 feet were available for the study. Of the 150 feet, 56 (37%) had a navicular BML, whereas 94 (63%) had not. Repeatability of SI ratio measurements was excellent for sagittal IRGE (R^2 = 98.4%), transverse STIR (R^2 = 98.9%), and sagittal STIR (R^2 = 99.2%) images.

Correlation of SI ratios obtained from both STIR planes was excellent (r = 0.96; $P < 0.001$; **Figure 2**), with the intercept value not significantly different from 0 and the slope not significantly different from 1. When agreement of SI measurements between both STIR planes was evaluated, there was no significant bias observed (bias, –0.08; 95% confidence interval, –0.49 to –0.33). The regression slope of the Bland-Altman test was not significantly (P = 0.54) different from 0, and intercept value was not significantly (P = 0.50) different from 0, allowing pooling of data. Pooling was performed by keeping data from the sole available plane or calculating the mean of values from both STIR planes.

In feet without a navicular BML, the SI ratios were smaller in the IRGE sequences, compared with the STIR sequences ($P < 0.001$; **Table 1**). The SI ratios were also significantly lower in feet without a navicular BML than those in feet with a BML, for both IRGE ($P < 0.001$) and STIR ($P < 0.001$) sequences.

Signal-to-noise ratio and CNR obtained from IRGE images were plotted against those obtained from STIR images. Signal-to-noise ratio and CNR of navicular bones with a BML correlated linearly ($P < 0.001$) in both sequences (r = 0.87 and r = 0.92, respectively; **Figure 3**). The slope was significantly ($P < 0.001$) < 1 for both the SNR and CNR. The SI ratio, SNR, and CNR were significantly ($P < 0.005$) higher in STIR images, compared with IRGE images, in feet with a navicular BML (Table 1; **Figures 4 and 5**).

All navicular BMLs were visually conspicuous in the STIR sequence. No navicular bone with a BML visible on STIR images had a CNR < 2. Applying that threshold to the IRGE sequence, BMLs were less conspicuous in 22 of 56 (39%) feet.

Discussion

Results confirmed the hypothesis that navicular BMLs were significantly less conspicuous on IRGE images, compared with STIR images. Both sequences have fundamentally low resolution and high contrast. Therefore, ill-defined non-cystic BML conspicuity relies almost solely on SI contrast between the lesion and normally fat-suppressed trabecular bone. Therefore, CNR is the most adequate parameter to assess lesion conspicuity in such sequences. The CNR is a difference of SNR between 2 tissues. Subtle contrast changes may be obscured on low SNR images,[1] and this is why both parameters should always be presented together. The SNR increases in proportion

to voxel volume and the square root of the number of excitations.[1]

In the context of human osteomyelitis assessed on a low-field system, IRGE sequences had a higher CNR than did the standard STIR sequences.[11] Furthermore, IRGE imaging was judged to be most beneficial along with T1-weighted GRE images to depict human traumatic bone marrow abnormalities, but with no comparison with standard STIR images.[12] Conversely, BMLs were less conspicuous in IRGE images, compared with STIR images, in our study. However, the highly linear correlation of CNR from both sequences likely indicates that both depicted the same pathological process but with different intrinsic capabilities.

The IRGE and STIR sequences had slightly different inversion times (75 vs 85 milliseconds, respectively), and this may certainly have affected the SNR and CNR results, although this is difficult to predict. These inversion times were initially defined as such by the manufacturer to provide subjectively similar normal tissue contrast. The manufacturer also proposes 2 additional versions of the STIR sequence with shorter and longer TI (named STIR + and STIR –, respectively) to increase fat suppression depending on limb temperature and age-related maturity of fat.[16] Only cases evaluated with standard STIR (constant TI, 85 milliseconds) images of diagnostic quality were included in this report for consistency, and cases with obvious fat suppression deficiency for any reason were excluded. There was probably less trabecular fat T1 relaxation time variation in our group of horses mainly composed of adult Warmbloods scanned in temperate zones, compared with young Thoroughbreds or horses scanned in tropical or polar zones. Moreover, the potential effect of varying the TI on BML conspicuity remains to be explored.

Furthermore, TE and TR were shorter in the IRGE sequences, potentially limiting the CNR, by reduced T2 weighting and incomplete longitudinal recovery, respectively, both of which could affect BML conspicuity. Conversely, spatial resolution was slightly (8%) higher in STIR images (voxel size, 5.8 mm^3), compared with IRGE images (voxel size, 6.3 mm^3), which might have been slightly detrimental to the STIR SNR but largely compensated for by a doubled number of excitations. Nevertheless, it was our goal to test the sequences as made available by the manufacturer. Increasing the TR of the IRGE sequence might improve the CNR but at the cost of a longer scan time, which would make it unrealistic for examining standing sedated horses. A longer TE would theoretically increase CNR but in fact would lead to either out-of-phase cancellation artifacts or even lower SNR due to lack of a rephasing pulse in GRE-type sequences. It is unusual to have a 90° flip angle in GRE-type sequences, which is similar as in the IRGE sequence. In most GRE sequences, decreasing the flip angle allows faster longitudinal recovery and therefore reduced scan time.[1] However, in IRGE, a long TR is necessary to wait for the inverted spins to recover. Therefore, a 90° flip angle can be used to maximize SNR.

Besides motion artifacts, other factors may contribute to suboptimal image quality in inversion recovery sequences, namely choice of an improper inversion time relative to the temperature of the limb or to the age of the horse may lead to deficient fat signal suppression.[16] In the study reported here, such horses with increased SI on STIR images but no manifestation of phase-cancellation artifact on T2*-weighted images were allocated to the no-BML group. However, it remains possible that data from horses with abnormal SI on T1-weighted and T2*-weighted images and increased SI in the fat-suppressed images due to a combination of a BML and lack of fat saturation might have altered the results by artificially increasing the measured SNR and CNR.

Other variables that may have affected SI measurements included foot and coil positioning relative to the isocenter of the magnet.[14] Imperfect positioning may have also resulted in insufficient fat suppression and therefore reduced CNR. As in all studies performed with low-resolution images, volume averaging causes artifacts (ie, with compact bone and synovial invaginations in our context); therefore, SI measurement errors have to be considered. However, both sequences, which had nearly identical spatial resolution, should have been affected in the same way with limited effect on their relative SNR and CNR. The navicular ROI size was chosen in a balance between representative measurements and volume-averaging effects. For several reasons, a navicular ROI of constant area over the region of maximal SI was drawn rather than an ROI of variable size delineating the BML. Typically, BMLs are ill-defined lesions, being inherently difficult to delineate. Besides, keeping ROI size constant facilitates comparison with bones without BMLs by means of similarly representative data. The lack of a sagittal STIR sequence for a portion of horses in this study was a limitation. However, the excellent results of the correlation and Bland-Altman tests allowed pooling data from both planes, which partially obviated this limitation. Furthermore, similar quantitative bone SI measurements can be obtained from 2 planes.[15] Because of potential piloting differences between sequences or the use of the transverse plane for some STIR images, navicular ROIs may not have been placed exactly at the same location for STIR and IRGE images. Rather, the ROI was always placed at the site of maximum SI because the goal was primarily to identify BMLs.

Although the results of the present study can be directly applied to the tested standing low-field system only, this is presently probably the most widely available system for horses. Furthermore, similar IRGE sequences can be obtained with many other low-field systems[11–13] and even some high-field systems. Questions are also raised about the potential BML conspicuity differences in commonly performed sequences such as STIR, fat-saturated T2-weighted fast spin echo, and fat-saturated spoiled gradient recalled images in high-field systems. In several studies, the use of STIR resulted in equal[17,18] or better[19–21] conspicuity for BML than the use of fat-saturated T2-weighted images, although both are still recommended in a recent review.[5] The question is also raised, although subjectively, for fat-saturated gradient echo-type sequences,[5,22] and this has been the object of strong debate in human medicine and veterinary research[4,23] and should definitely warrant further study in equine patients.

In daily clinical practice, CNR measurements are not routinely performed. The present study provided objective quantitative data about intrinsic contrast res-

olution capabilities of the tested sequences. It was not the authors' objective to provide a subjective observer assessment with reading performance (sensitivity and specificity) about the presence or absence of BMLs. Indeed, this pathological process is likely gradual and the threshold for human-eye depiction of such a lesion is likely operator dependent and variable according to the working environment and level of experience with a particular system or sequence. Measuring the performance of 1 or a few readers would be of limited value in this context and was not performed in studies[11,12,17–21,24,25] that used the same design. Furthermore, the absence of a definite gold standard in this context actually precludes calculation of sensitivity and specificity. Finally, there is no reported CNR below which the human eye is more likely to fail at depicting a lesion.

Our definition of a definite BML was based on other observations in equine patients,[8,14] with a combination of SI alterations in several sequences. Specifically, the use of out-of-phase T2*-weighted sequences has been reported in the human literature in the context of bone trauma.[25,26] However, it must be acknowledged that early BMLs or BMLs of mild degree might be visible in the most fluid-sensitive STIR images only. Such cases may have been erroneously allocated to the non-BML group of the present study. However, a potentially restrictive definition of BML was intentionally preferred to ascertain their presence to perform the comparison. Investigating the ability of the 2 sequences tested to detect such mild BMLs would require a gold-standard test for confirmation. Histologic examination results were not available in this clinical case series, as in most human studies[11,12,17–21,25] that used the same design. Given the extreme variability of microscopic findings[2,5,27,28] and lack of consensus for histologic examination of BMLs, histologic examination has its own limitations in this context.

Interestingly, the mean SI ratio between the navicular bone and the middle phalanx in feet without a definite BML was slightly > 1 and significantly different in both sequences. Again, this may be actually due to a small proportion of unrecognized BMLs in the non-BML group. However, the prevalence of definite navicular BMLs in this study (37%) compared favorably with the reported prevalence in a high-field system (26% to 39%).[29,30] Furthermore, in a recent study,[16] the T1 values in the navicular trabecular bone and in the middle phalanx were seemingly different, although the difference was not tested statistically and the potential presence of lesions was not verified by any mean. Therefore, a strict SI ratio of 1 should not necessarily be expected in normal bones and this ratio is also possibly dependent on sequence parameters

Caution should be observed when an IRGE sequence is used to detect BMLs in equine digits because these are likely to appear much less conspicuously, compared with a standard STIR sequence. An apparently normal bone SI in that sequence certainly does not rule out the presence of a BML, and STIR sequences should be included in a standard protocol. The IRGE sequence might be useful in circumstances when low-quality STIR images are obtained in a moving standing horse, but this warrants further investigations.

a. EQ2, Hallmarq Veterinary Imaging, Guildford, Surrey, England.
b. E-Film 2.1.2, Merge Healthcare, Milwaukee, Wis.
c. MedCalc, version 12.1.4.0, MedCalc Software, Mariakerke, Belgium.
d. SAS, version 9.1, SAS Institute Inc, Cary, NC.

References

1. McRobbie DW, Moore EA, Graves MJ, et al. *MRI from picture to proton*. 2nd ed. Cambridge, England: Cambridge University Press, 2007.
2. Zanetti M, Bruder E, Romero J, et al. Bone marrow edema pattern in osteoarthritic knees: correlation between MR imaging and histologic findings. *Radiology* 2000;215:835–840.
3. Conaghan PG, Felson D, Gold G, et al. MRI and non-cartilaginous structures in knee osteoarthritis. *Osteoarthritis Cartilage* 2006;14:A87–A94.
4. d'Anjou MA, Troncy E, Moreau M, et al. Temporal assessment of bone marrow lesions on magnetic resonance imaging in a canine model of knee osteoarthritis: impact of sequence selection. *Osteoarthritis Cartilage* 2008;16:1307–1311.
5. Roemer FW, Frobell R, Hunter DJ, et al. MRI-detected subchondral bone marrow signal alterations of the knee joint: terminology, imaging appearance, relevance and radiological differential diagnosis. *Osteoarthritis Cartilage* 2009;17:1115–1131.
6. Sampson SN, Schneider RK, Gavin PR, et al. Magnetic resonance imaging findings in horses with recent onset navicular syndrome but without radiographic abnormalities. *Vet Radiol Ultrasound* 2009;50:339–346.
7. Dyson SJ, Murray R, Schramme MC. Lameness associated with foot pain: results of magnetic resonance imaging in 199 horses and response to treatment. *Equine Vet J* 2005;37:113–121.
8. Olive J, Mair TS, Charles B. Use of standing low-field magnetic resonance imaging to diagnose middle phalanx bone marrow lesions in horses. *Equine Vet Educ* 2009;21:116–123.
9. Holowinski M, Judy C, Saveraid T, et al. Resolution of lesions on STIR images is associated with improved lameness status in horses. *Vet Radiol Ultrasound* 2010;51:479–484.
10. Jenner F, Kirker-Head C. Core decompression of the equine navicular bone: an in vivo study in healthy horses. *Vet Surg* 2011;40:151–162.
11. Bonel H, Helmberger T, Geiss HC, et al. Comparison of sequences for depicting bone marrow alterations in osteomyelitis applied in a low field strength magnetic resonance imaging system. *MAGMA* 1998;7:1–8.
12. Bonel H, Helmberger T, Sittek H, et al. A comparison of pulse sequences in the detection of post-traumatic bone marrow abnormalities at low field strength MRI. *Skeletal Radiol* 1997;26:538–543.
13. Piola V, Posch B, Radke H, et al. Magnetic resonance imaging features of canine incomplete humeral condyle ossification. *Vet Radiol Ultrasound* 2012;53:560–565.
14. Murray RC, Werpy N. Image interpretation and artefacts. In: Murray RC, ed. *Equine MRI*. Ames, Iowa: Wiley-Blackwell, 2011;101–113.
15. Olive J, d'Anjou MA, Alexander K, et al. Correlation of signal attenuation–based quantitative magnetic resonance imaging with quantitative computed tomographic measurements of subchondral bone mineral density in metacarpophalangeal joints of horses. *Am J Vet Res* 2010;71:412–420.
16. Adrian AM, Koene M, Roberts S, et al. The influence of temperature and age on the T1 relaxation time of the equine distal limb. *Vet Radiol Ultrasound* 2012;53:296–303.
17. Wohlgemuth WA, Roemer FW, Bohndorf K. Short tau inversion recovery and three-point Dixon water-fat separation sequences in acute traumatic bone fractures at open 0.35 Tesla MRI. *Skeletal Radiol* 2002;31:343–348.
18. Arndt WF III, Truax AL, Barnett FM, et al. MR diagnosis of bone contusions of the knee: comparison of coronal T2-weighted fast spin-echo with fat saturation and fast spin-echo STIR images with conventional STIR images. *AJR Am J Roentgenol* 1996;166:119–124.
19. Mirowitz SA, Apicella P, Reinus WR, et al. MR imaging of bone marrow lesions: relative conspicuousness on T1-weighted, fat-

suppressed T2-weighted, and STIR images. *AJR Am J Roentgenol* 1994;162:215–221.
20. Pui MH, Goh PS, Choo HF, et al. Magnetic resonance imaging of musculoskeletal lesions: comparison of three fat-saturation pulse sequences. *Australas Radiol* 1997;41:99–102.
21. Pui MH, Chang SK. Comparison of inversion recovery fast spin-echo (FSE) with T2-weighted fat-saturated FSE and T1-weighted MR imaging in bone marrow lesion detection. *Skeletal Radiol* 1996;25:149–152.
22. Hilfiker P, Zanetti M, Debatin JF, et al. Fast spin-echo inversion-recovery imaging versus fast T2-weighted spin-echo imaging in bone marrow abnormalities. *Invest Radiol* 1995;30:110–114.
23. Yoshioka H, Stevens K, Hargreaves BA, et al. Magnetic resonance imaging of articular cartilage of the knee: comparison between fat-suppressed three-dimensional SPGR imaging, fat-suppressed FSE imaging, and fat suppressed three-dimensional DEFT imaging, and correlation with arthroscopy. *J Magn Reson Imaging* 2004;20:857–864.
24. Roemer FW, Hunter DJ, Guermazi A. MRI-based semiquantitative assessment of subchondral bone marrow lesions in osteoarthritis research. *Osteoarthritis Cartilage* 2009;17:414–415.
25. Zampa V, Carafoli D, Grassi L, et al. Usefulness of opposed-phase gradient-echo technique in the diagnosis of occult lesions of the knee and comparison with traditional T1-weight sequences (in-phase) [in Italian]. *Radiol Med* 2000;99:31–35.
26. Vande Berg BC, Malghem J, Lecouvet FE, et al. Classification and detection of bone marrow lesions with magnetic resonance imaging. *Skeletal Radiol* 1998;27:529–545.
27. Murray RC, Blunden TS, Schramme MC, et al. How does magnetic resonance imaging represent histologic findings in the equine digit? *Vet Radiol Ultrasound* 2006;47:17–31.
28. Dyson S, Blunden T, Murray R. Comparison between magnetic resonance imaging and histological findings in the navicular bone of horses with foot pain. *Equine Vet J* 2012;44:692–698.
29. Dyson S, Murray R. Use of concurrent scintigraphic and magnetic resonance imaging evaluation to improve understanding of the pathogenesis of injury of the podotrochlear apparatus. *Equine Vet J* 2007;39:365–369.
30. Dyson SJ, Murray RC, Schramme MC, et al. Magnetic resonance imaging in 18 horses with palmar foot pain, in *Proceedings*. 48th Am Assoc Equine Pract Annu Conv 2002;145–154.